JCTC Journal of Chemical Theory and Computation

Lewis Acid and Substituent Effects on the Molecular Mechanism for the Nazarov Reaction of Penta-1,4-dien-3-one and Derivatives. A Topological Analysis Based on the Combined Use of Electron Localization Function and Catastrophe Theory†

Victor Polo and Juan Andrés*

Departamento de Química Física y Analítica, Universidad Jaime I, Apartado 224, 12080, Castellón, Spain

Received February 5, 2007

Abstract: The joint use of the topological analysis provided by the electron localization function (ELF) and catastrophe theory (CT), at the B3LYP/6-31G(d) calculation level, allows us to examine the Lewis acid (protonation H^+ and presence of BH_3) and the role of an electron donor substituent ($-OCH_3$) at α and β positions along the course of the molecular mechanism for the Nazarov rearrangement of penta-1,4-dien-3-one and eight derivatives. The progress of the reaction is monitored by the changes of the ELF structural stability domains (SSDs), each change being controlled by a turning point derived from CT. These SSDs and the corresponding turning points are associated with a sequence of elementary chemical steps. Along the cyclization path of penta-1,4-diene-3-one, four SSDs as well as three turning points (cusp1−fold1−cusp2) have been characterized. The first and second SSDs correspond to a polarization of the C−O bond and electronic redistribution among the C−C bonds, respectively, and they can be associated with the formation of an oxyallyl structure. The third and fourth SSDs can be assigned to the ring closure process. Protonation of the oxygen atom shifts the reactive directly into the second SSD, greatly reducing the activation and reaction energies. The electronic effects due to Lewis acids and electron donor substituents have been rationalized in terms of calculations of mesomeric structures from ELF basin populations. The combination of Lewis acids together with α and β $-OCH_3$ substitutions renders a cooperative and competitive effect on activation and reaction free energies, respectively.

1. Introduction

One of the fundamental issues of the theoretical descriptions of chemical reactivity stands on the complete understanding of reaction mechanisms. The rearrangements among electron pairs along the pathway connecting the reactives to the products can be perturbed in multiple ways; that is, catalysts can accelerate the reaction toward a desired product. The analysis of the electron density enables the extraction of information from the wave function in a form that is readily interpretable with reference to physicochemical properties of a molecule. Modern techniques for the analysis of chemical bonding have been developed recently on the basis of properties of the topological analysis of the electron density, as the atoms in molecules of Bader[1] or the electron localization function (ELF),[2] developed for the study of electron pairing by Silvi and Savin.[3] Topological analysis of ELF enables the chemist to condense the information succinctly to interpret diverse bonding situations, such as the recently defined bond shift,[4] (homo-) aromaticity,[5] or the

† Dedicated to Professor Dennis R. Salahub on the occasion of his 60th birthday.

* Corresponding author phone: (+34) 964-728071; fax: (+34) 964-728066; e-mail: andres@qfa.uji.es.

10.1021/ct7000304 CCC: $37.00
Published on Web 04/13/2007

Scheme 1. Reactions Studied in This Work

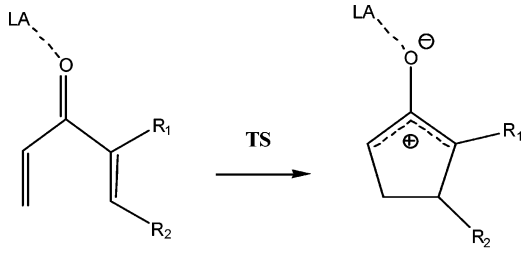

	LA: -	LA: BH_3	LA: H^+
R_1=-H; R_2=H	(1)	(2)	(3)
R_1=-OCH_3; R_2=H	(4)	(5)	(6)
R_1=-H; R_2=-OCH_3	(7)	(8)	(9)

nature of the bridge bond in propellanes.[6] A further development was introduced by the bonding evolution theory (BET)[7] which combined the ELF and Thom's catastrophe theory (CT)[8] for the analysis of the creation/annihilation of ELF basins. According to BET, the rigorous definition of electron pairing provided by ELF[9] and the identification and characterization of turning points along the reaction pathway can be associated into well-defined chemical events (bond breaking/forming processes, creation/annihilation of lone pairs, etc.); therefore, an innovative understanding of the corresponding molecular mechanism associated with chemical rearrangements can been reached. In this regard, several papers have been presented to map out chemical reactions.[10] Although this analysis relies on a "static" description of the reaction path, Adamo and co-workers[11] have investigated using ab initio molecular dynamics bond breaking and formation processes, and they found that the ELF topology yielded equivalent results to the "static" description.

Electrocyclizations are powerful transformations in organic synthesis.[12] One type of electrocyclic reaction is a 4π-electron process known as the Nazarov cyclization[13−15] involving the conversion of a divinyl ketone to an oxyallyl five-membered ring (see Scheme 1). Traditionally, harsh reaction conditions with strong acids or high temperatures were needed. Recently, the potential applications of the Nazarov reaction in synthesis have grown enormously by the use of Lewis acids as catalysts, complexation with chiral metals for asymmetric synthesis,[16] and the wide variety of substrates as well as procedures that allow carrying out of the "interrupted" Nazarov reaction.[17]

In the Nazarov reaction, the key step is the cyclization of a 4π-electron system through a conrotatory (under thermal conditions) electrocyclic process to form a five-membered ring. Although the mechanism of the Nazarov reaction is well-known at an experimental[15] as well as theoretical level,[18] our understanding is far from complete. It is well-known that three electronic factors control the progress of the cyclization, namely, (a) protonation of the oxygen or complexation to a mild Lewis acid (LA) catalyzes the cyclization,[19] (b) α-electron-donating substituents accelerate the reaction,[20] and (c) β-electron-donating substituents accelerate the retro-Nazarov ring cleavage.[21] The current work is devoted to investigate how and where the bond breaking/forming processes and the corresponding electronic distributions take place along the molecular mechanisms of the Nazarov reaction of diallyl ketones to obtain five-membered rings from the perspective of the ELF and CT analysis, taking into account the a−c factors described above. A set of 3 × 3 reactions have been calculated (see Scheme 1) considering the protonation, H^+, of the oxygen atom of the C_1-O_6 group and the presence of BH_3, as strong and moderate LAs, respectively, and metoxy ($-OCH_3$) as an electron-donating group in the α (at C_2 atom) and β (at C_3 atom) positions. The effect of the LA on the cyclization of penta-1,4-diene-3-one is shown in reactions 1−3; the LA combined to an α- or β-metoxy group in reactions 4−6 and 7−9, respectively.

The structure of the article is arranged as follows: the computational methods are presented in section 2. The results and discussion section is divided in four parts. First, in order to understand the electronic structure of penta-1,4-diene-3-one and its oxyallyl ring, the weights of the Lewis resonance structures will be determined on the basis of ELF basin populations. Second, the reaction mechanism for the cyclization process for the neutral and protonated species, reactions 1 and 3, respectively, will be discussed by means of the combined use of ELF and CT analysis. Third, the electron-donating capability of the α and β $-OCH_3$ groups will be shown by means of trends of ELF basin populations for the stationary points of reactions 1, 4, and 7. Fourth, the electronic effects due to LA and $-OCH_3$ substitution will be related to the calculated activation and reaction free energies. A brief concluding remarks section closes the article.

2. Theoretical Methods

The geometry optimizations and electronic structure calculations were carried out by the Gaussian 03 program.[22] Structures were optimized using the B3LYP hybrid exchange-correlation potential[23] together with the 6-31G(d) basis set.[24] For the sake of comparison, reaction 7 is calculated using the 6-31+G(d) basis set, because the oxyallyl ring structure cannot be found without diffuse functions. Stationary points on the potential energy surface were characterized by harmonic analysis using the same theoretical level as used in the optimization. The B3LYP activation energy is in good agreement with experimental data and previous works using ab initio[18a−d] or DFT methods.[18e,f] In the present work, reactives are connected to the transition structure (TS) by means of intrinsic reaction coordinate (IRC) calculations, using the method proposed by Fukui[25] and developed by Gonzalez and Schlegel.[26] A step size of 0.1 amu$^{1/2}$ bohr and the calcfc option as implemented in Gaussian 03 were employed for the IRC calculations.

The topological analysis of the ELF function, η(r), has been proved to be a useful tool to investigate the electronic structure and chemical reactivity of molecular systems.[27] An exploration of the mathematical properties of η(r) enables a partition of the molecular position space in basins of attractors, which present a one-to-one correspondence with chemical local objects such as bonds and lone pairs. These

basins are either core basins, C(X), or valence basins, V(X,...), belonging to the outermost shell and characterized by their coordination number with core basins, which is called the synaptic order.[28] From a quantitative point of view, the electron density method can be integrated over the basins to provide the basin populations, $\bar{N}$. Along the reaction pathway, the change of the nuclear coordinates can lead to different topologies of the ELF. Thus, the reaction path is divided into subsets with the same ELF topology, and they are called structural stability domains (SSDs). Two consecutive SSDs are connected by a turning or bifurcation point which is characterized by a zero value of the Hessian matrix of the ELF. Each catastrophe transforms the overall topology in such a way that the Poincaré−Hopf relation is fulfilled. Three types of bifurcation catastrophes have been found so far in the study of chemical reactivity: (i) the fold catastrophe, corresponding to the creation or the annihilation of two critical points of different parity; for example, a wandering point gives rise to an attractor (index 0) and a saddle point of index 1; (ii) the cusp catastrophe, which transforms one critical point into three (and vice versa) such as in the formation or the breaking of a covalent bond; and (iii) the elliptic umbilic in which the index of a critical point changes by two. More information about the ELF and CT analysis of the chemical reactivity can be found elsewhere.[7] Technically, the Kohn−Sham orbitals were obtained for each point of the calculated IRC path, and the ELF analysis was carried out using a cubical grid of a step size smaller than 0.1 bohr, employing the TopMod package of programs.[29] The graphical representation was obtained using the MOLEKEL program.[30]

3. Results and Discussion

3.1. Calculation of Lewis Resonance Structures for Penta-1,4-diene-3-one and Its Oxyallyl Ring. The analysis based on the ELF topology allows quantification of the resonance structures proposed in Denmark's pioneering study of substituent effects in the Nazarov reaction,[20] even for the neutral species. Hence, for penta-1,4-diene-3-one (R1), the ELF shows two lone pairs represented by $V_{1,2}(O_6)$ basins with an integrated population of 2.62 e each. The C−O bond is strongly polarized toward the O atom, and its population is 2.35 e. This type of bond corresponds to a charge-shift type due to the different electronegativity of the atoms, where some amount of the bond electron density is shifted toward the oxygen lone pairs. Single (double) C−C bonds are represented by one (two) disynaptic basin(s) between the corresponding atoms with typical populations for this type of basin. The product, the oxyallyl ring (P1), presents a larger population on the two O_6 lone pairs, 2.82 e each, and a smaller C−O bond population, 2.05 e. The C_1-C_2 and C_1-C_5 basins present a population intermediate between a single and double bond, 2.70 e. The C−C bonds adjacent to C_1-C_2 and C_1-C_5 are slightly more populated than single bonds.

The basin populations of reactives and products correspond to a superposition of Lewis resonance structures R1a−R1d and P1a−P1b as depicted in Schemes 2 and 3, respectively. Structure R1a has three double bonds and all atoms remain neutral, whereas R1b−R1d are zwitterionic structures, the negative and positive charge being located on the oxygen atom and on the C_1, C_3, and C_4 carbon atoms, respectively. The corresponding ELF basin populations and the number of electrons for each resonance structure are gathered in Table 1a and b, respectively. Fitting the resonance weights to the basin populations yields the following results: $w_{R1a} = 0.24$, $w_{R1b} = 0.40$, $w_{R1c} = 0.18$, and $w_{R1d} = 0.18$. Although the carbocation is delocalized between C_1, C_3, and C_4, the weight of R1b equals the sum of R1c and R1d. The oxyallyl ring P1 can be reasonably described by the superposition of just two distinct resonance forms P1a and P1b with equal weights.

Scheme 2. Proposed Lewis Resonance Forms for Penta-1,4-diene-3-one (R1)

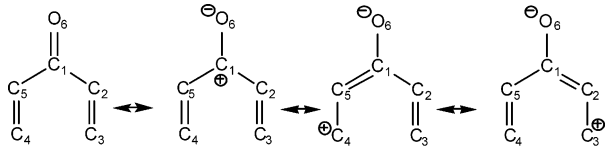

Scheme 3. Proposed Lewis Resonance Forms for the Oxyallyl Ring (P1)

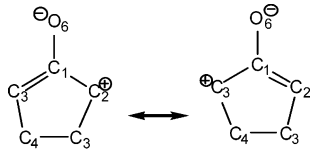

Table 1. Basin Populations ($\bar{N}$) and Number of Electrons Per Basin for Each Lewis Resonance Form of (a) R1 and (b) P1

(a) R1

	ELF		Lewis structures			
	$\bar{N}$	$\bar{N}$ scaled[a]	R1a	R1b	R1c	R1d
$V(C_3,C_4)$	2.21	2.35	2	2	4	2
$V(C_4,C_5)$	2.21	2.35	2	2	2	4
$V(C_4,O_6)$	2.35	2.50	4	2	2	2
$V(O_6)$	5.23	5.56	4	6	6	6
$V(C_2,C_3)$	3.41	3.62	4	4	2	4
$V(C_1,C_5)$	3.41	3.62	4	4	4	2

(b) P1

	ELF		Lewis structures	
	$\bar{N}$	$\bar{N}$ scaled[b]	P1a	P1b
$V(C_1,C_2)$	2.71	2.89	2	4
$V(C_1,C_5)$	2.71	2.89	4	2
$V(C_1,O_6)$	2.05	2.19	2	2
$V(O_6)$	5.64	6.02	6	6

[a] Scale factor of $20/(\sum \bar{N}) = 1.06$. [b] Scale factor of $14/(\sum \bar{N}) = 1.03$.

3.2. A Combined Used of the ELF and Catastrophe Theory Analysis of the Protonation Effect in Nazarov's Cyclization. The reaction paths connecting R−TS−P calculated using the IRC method for reactions 1 and 3 are shown in Figure 1.[31] Below the potential energy profile, a schematic representation of the change of topology of ELF basins using Lewis type structures is depicted. Reaction 1 presents four

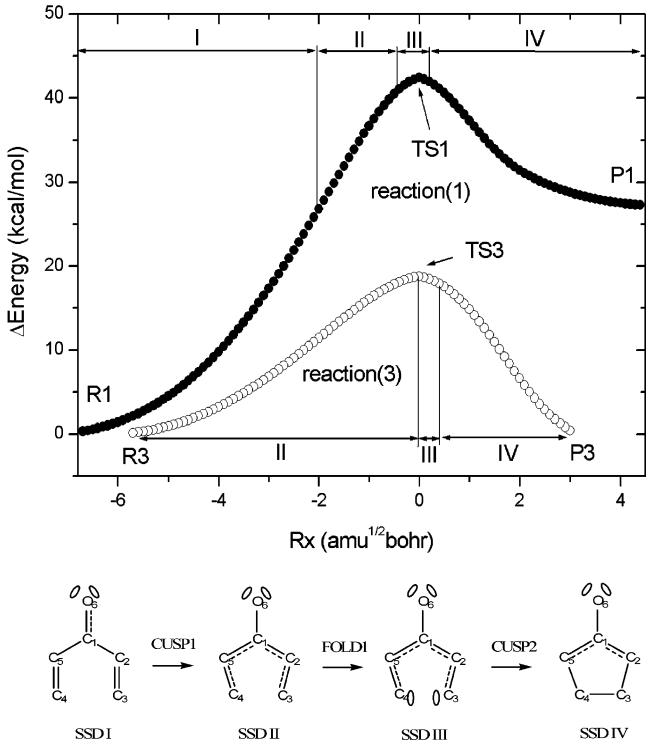

Figure 1. B3LYP/6-31G(d) calculated energy profiles for the Nazarov cyclizations 1 and 3 (energy values relative to the respective reactive) calculated by means of the IRC method, with a step size of 0.1 (amu$^{1/2}$ bohr). Below the graph, a schematic representation of the Lewis resonance forms for each SSD is depicted from the perspective of the ELF analysis (full lines and ellipses representing disynaptic and monosynaptic basins, respectively, while dotted lines indicate a large basin population).

SSDs (I−IV) connected by cusp1, fold1, and cusp2 turning points, respectively. A snapshot of the ELF for each SSD is displayed in Figure 2. The protonated reaction (reaction 3) presents neither the first SSD nor the cusp1 turning point, the other ELF topological features being identical to those of reaction 1. The populations for valence basins at the first and last points of each SSD of reactions 1 and 3 are gathered in Tables 2 and 3. In addition, the distance rC$_3$−C$_4$ and the increment of energy along each SSD are also included.

The first SSD (I) of the reaction path of reaction 1 is characterized by the absence of transference of electronic charge between the ELF basins. However, there are substantial geometrical changes due to the conrotatory movement of both CH_2 terminal units. This SSD is the most costly energetically (25.83 kcal/mol), and a polarization of the C$_1$−O$_6$ bond is appreciated by the increment of 0.13 e of the basins associated with the lone pairs of the O$_6$ atom. The second SSD (II) of reaction 1 starts by the transformation of the degenerate disynaptic $V_{1,2}(C_{i=2,4},C_{j=3,5})$ into a unique $V(C_{i=2,4},C_{j=3,4})$ basin by means of a cusp-type turning point, cusp2. The rotation of the CH_2 units along the first SSD leads to the merge of the two basins corresponding to the terminal double bonds into a single one. Reaction 3 starts in this SSD; the protonation of O$_6$ creates a V(O$_6$,H) basin of 1.77 e; besides, the population of the lone pair of O$_6$ is 4.14 e, and the $\bar{N}$[V(C$_1$,O$_6$)] basin is decreased to 1.77 e. There are also substantial changes on the C−C bond basins; whereas $V(C_{i=1,1},C_{j=2,5})$ and V(C$_1$,C$_5$) increase the population to 2.38 e, $V(C_{i=2,3},C_{j=3,4})$ is connected by one disynaptic basin with a population of 3.23 e. Hence, the ELF topology of R3 is equivalent to the corresponding one at the second SSD of reaction 1. Along the second step, there is a noticeable charge-transfer process from the new basin $V(C_{i=2,4},C_{j=3,5})$, −0.23 e (reaction 1) and −0.55 e (reaction 3), to the $V(C_{i=1,1},C_{j=2,5})$ basins, 0.20 e (reaction 1) and 0.27 e (reaction 3), and V(O$_6$), 0.14 e (reaction 1) and 0.20 e (reaction 3). This electronic rearrangement is accompanied by an increment of the energy of 14.66 and 18.83 kcal/mol, for reactions 1 and 3, respectively.

The third SSD (III) begins shortly before the TS1 is reached, at Rx = −0.30 amu$^{1/2}$ bohr, and at the same point as TS3. According to Thom's catastrophe theory, it is a fold-type turning point, fold1, where two monosynaptic basins on the terminal carbons are created [V(C$_3$) and V(C$_4$)]. Hence, terminal carbons are now connected by two monosynaptic basins, and this type of interaction between atoms has been termed as a "proto-covalent" bond, and it takes place immediately before (or after) the formation (breaking) of a covalent bond. It is interesting to remark that TS1 and TS3 belong to different SSDs; thus, examination of the TS instead of the progress along the reaction path could be misleading. The only transference of electron density among ELF basins occurs from $V(C_{i=2,4},C_{j=3,5})$ to the newly created $V(C_{i=3,4})$.

The last step starts at Rx = +0.20 (reaction 1) and +0.50 (reaction 3) amu$^{1/2}$ bohr, and it corresponds to the creation of a disynaptic basin V(C$_3$,C$_4$) from the monosynaptic basins V(C$_3$) and V(C$_4$) by means of a cusp-type turning point; in other words, the ring is closed by the formation of a covalent bond between the terminal atoms. Along the fourth SSD (IV), there is an energy stabilization of 15.03 and 6.28 kcal/mol for reactions 1 and 3, respectively, and the new basin commences with a low population (0.93 e), and it increases until a population typical of a single C−C bond is reached, 1.83 e (reaction 1) and 1.84 e (reaction 3).

In summary, although the cyclization from the penta-1,3-diene-4-one to the corresponding oxyallyl ring takes place along one TS, the individual electronic rearrangements do not take place simultaneously but along four well-defined SSDs of the ELF separated by cusp1−fold1−cusp2 turning points. The reaction starts by the formation of the oxyallyl structure, while the ring closure takes place in the last part of the reaction. The presence of a LA, cases 2 and 3, stabilizes the negative partial charge of O$_6$ and shifts electron density from the terminal double bonds to the single bonds and from the C$_1$−O$_6$ bond to O$_6$ lone pairs. As a consequence of these electronic rearrangements, the reaction path of 3, H^+ protonation, begins directly at the second SSD avoiding the first (and energetically very costly) SSD of reaction 1. In SSD II, there is an electronic transfer process from terminal C−C bonds to C$_1$−C$_2$ and C$_1$−C$_5$. The third step starts in the vicinities of the TS, and it is characterized by the proto-covalent bond between terminal C atoms. Finally, the ring-closure process takes place by the formation of the covalent bond C$_3$−C$_4$.

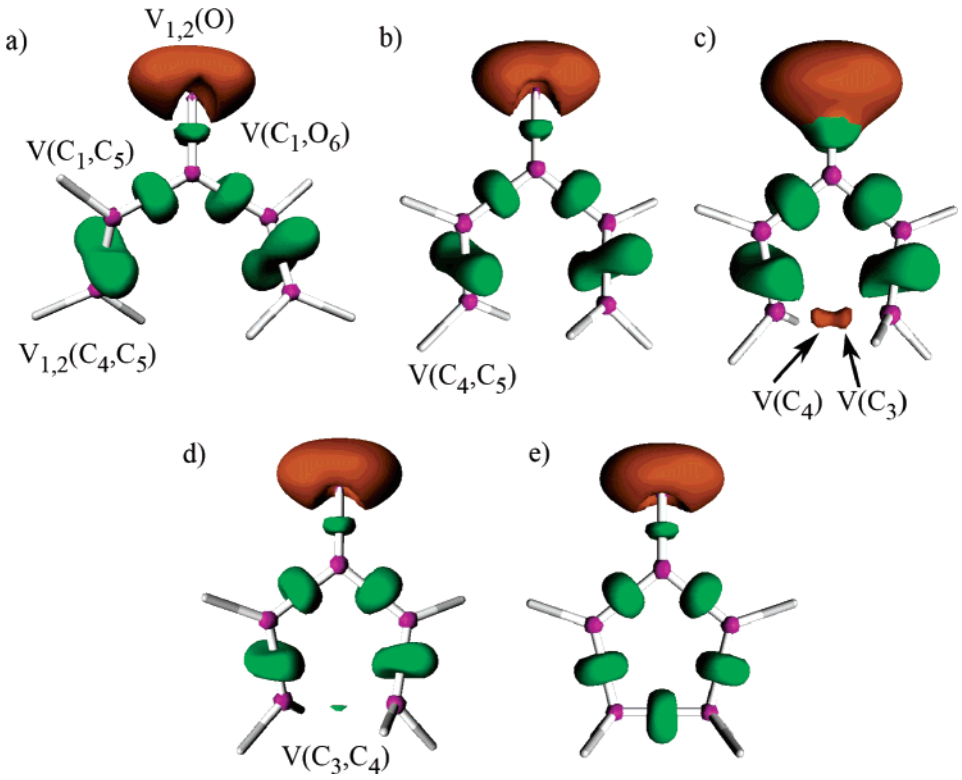

Figure 2. Snapshots of ELF localization domains ($\eta = 0.8$ isosurface, except 0.75 for c) for (a) reactive (SSD I), (b) Rx = −0.40 (SSD II), (c) TS (SSD III), (d) Rx = −0.20 (SSD IV), and (e) product (SSD IV). Basin color legend: purple for core, orange for monosynaptic, and green for disynaptic. Hydrogenated basins are omitted for clarity.

Table 2. Rx (in amu$^{1/2}$ bohr), Increments of Energy within Each SSD ΔE^a (in kcal/mol), rC$_3$−C$_4$ Distance (in Å), and Integrated Electron Populations for Valence ELF Basins of Reaction 1 Calculated for the Initial and Final Points of Each SSD Identified on the Energy Reaction Profile Using the ELF Analysis

SSD	I		II		III			IV	
Rx	R	−2.0	−1.9	−0.4	−0.3	TS(0.0)	0.1	0.2	P
rC$_3$−C$_4$	3.229	2.319	2.302	2.035	2.018	1−949	1.916	1.898	1.541
ΔE	25.83		14.66		1.74			−15.03	
V(C$_1$,C$_2$)	2.21	2.29	2.31	2.51	2.53	2.56	2.61	2.64	2.74
V(C$_1$,O$_6$)	2.35	2.29	2.28	2.16	2.14	2.15	2.14	2.12	2.05
V(O$_6$)	2.62/2.62	2.68/2.68	2.68/2.68	2.75/2.75	2.76/2.76	2.75/2.75	2.76/2.76	2.77/2.77	2.82/2.82
V(C$_3$,C$_4$)								0.93	1.83
V(C$_3$)					0.22	0.36	0.44		
V(C$_4$)					0.22	0.36	0.44		
V$_{1,2}$(C$_{2,4}$,C$_{3,5}$)	1.63/1.78	1.63/1.65	3.27	3.04	2.82	2.65	2.55	2.51	2.12
V(H$_1$,C$_{3,4}$)	2.1	2.11	2.12	2.11	2.09	2.05	2.04	2.03	1.95
V(H$_6$,C$_{3,4}$)	2.09	2.11	2.11	2.1	2.1	2.1	2.1	2.09	1.97

[a] For each SSD, $\Delta E = E$(final) − E(initial).

3.3. ELF Analysis of −OCH$_3$ Substituent Effects on the Nazarov Cyclization. The ELF analysis of the reaction path for reactions 4 and 7, with an −OCH$_3$ in α and β positions, respectively, shows the same sequence of SSDs and turning points as the unsubstituted reaction (reaction 1). The corresponding stationary points (R, TS, and P) of these three reactions (1, 4, and 7) have the same ELF topology. Therefore, a comparative analysis of their differences on the basin populations, and their trends, can be carried out in order to understand the −OCH$_3$ effect on the electronic rearrangements of Nazarov cyclization. The data of ELF populations for R, TS, and P of reactions 1, 4, and 7 are gathered in Table 4.

A comparative analysis of the progress of these reactions (4 and 7) with respect to the parent model (reaction 1) points out a similar behavior. However, there are two main differences between reactions 4 and 1: first, there is a larger increment of $\bar{N}$[V(C$_1$,C$_5$)] for reaction 4 than in reaction 1; second, there is a transfer of electron charge from the lone pairs of O$_7$ to the C$_2$−O$_7$ bond. Hence, V(O$_7$) decreases its population, R4 (4.59 e), TS4 (4.41 e), and P4 (4.03 e), while $\bar{N}$[V(C$_2$,O$_7$)] increases for R4 (1.50 e), TS4 (1.63 e), and P4 (1.89 e). Both differences may be interpreted in terms of the resonance Lewis structures discussed in section 3.1. Whether for P1 both Lewis structures, a and b, have equal weight, for P4, the weight of the corresponding P4a is larger

Table 3. Rx (in amu$^{1/2}$ bohr), SSD Increment of Energy ΔE^a (in kcal/mol), rC$_3$−C$_4$ Distance, and Integrated Electron Populations for Valence ELF Basins of Reaction 3 Calculated for the Initial and Final Points of Each SSD Identified on the Energy Reaction Profile Using the ELF Analysis

SSD	II		III		IV	
Rx	R	TS (0.0)	0.1	0.5	0.6	P
rC$_3$−C$_4$	3.183	2.108	2.074	2.003	1.985	1.536
ΔE	18.83		6.28		6.28	
V(C$_1$,C$_2$)	2.38	2.65	2.66	2.69	2.69	2.71
V(C$_1$,O$_6$)	1.77	1.65	1.65	1.64	1.65	1.61
V(O$_6$)	4.14	4.34	4.35	4.38	4.38	2.16/2.31
V(O$_6$,H)	1.77	1.71	1.7	1.69	1.68	1.64
V(C$_3$,C$_4$)					0.69	1.84
V(C$_3$)			0.19	0.31		
V(C$_4$)			0.19	0.31		
V1(C$_{2,4}$,C$_{3,5}$)	3.23	2.68	2.61	2.49	2.46	2.09
V(H$_1$,C$_{3,4}$)	2.1	2.13	2.13	2.14	2.15	2.16
V(H$_6$,C$_{3,4}$)	2.09	2.22	2.08	2.04	2.03	1.92

[a] For each SSD $\Delta E = E$(final) − E(initial).

than P4b due to the electron donation of the −OCH$_3$ group. A transfer of electronic charge from the O$_7$ lone pairs to the C$_2$−C$_7$ bond around 0.40 e is sensed, stabilizing the cation at the C$_2$ atom. Hence, the analysis of ELF is in full agreement with Denmark's model, giving a quantitative measure of the electron-donating effect.

The ELF basin population trends observed on the stationary points of reaction 7 are more similar to those of reaction 1 than in the case of reaction 4. However, analysis of the behavior of $\bar{N}$[V(C$_3$,O$_7$)] and $\bar{N}$[V(O$_7$)] basins for R7−TS7−P7 structures shows a transfer of electronic charge of 0.22 e (approximately) from V(C$_3$,O$_7$) to V(O$_7$) basins. Therefore, the −OCH$_3$ electron-donating effect at the C2 and C3 positions go in opposite directions. However, the magnitude of the electron donation from the lone pairs of O$_7$ to the C$_3$−O$_7$ bond in reaction 7 is smaller than in reaction 4, and the role of this electronic transfer into the basins participating on the cyclization process cannot be clearly distinguished. Therefore, the electron-donating effect of the β −OCH$_3$ group should stabilize R7 and TS7 (less) with respect to P7, which also agrees with Denmark's model predicting that β-electron-donating groups should stabilize the pentadiene cation, discouraging cyclization. Comparison between TS1 and TS7 reveals a larger $\bar{N}$[V(C$_1$,C$_2$)] for the latter, 0.23 e, suggesting a more efficient electronic charge process from V(C$_2$,C$_3$) to V(C$_1$,C$_2$) due to the presence of the −OCH$_3$ group. Also, the populations of V(C$_3$) and V(C$_4$) basins at TS7 are not identical, indicating that the bond formation is not a pure homolytical process.

3.4. Does the Presence of Lewis Acid and α,β −OCH$_3$ Substitution Yield a Cooperative or a Competitive Effect? Once the changes on the electronic structure due to LA−protonation (H$^+$) and presence of BH$_3$−and α,β metoxy substitution have been analyzed using the ELF analysis, we will relate these observations to the thermochemical data calculated at the B3LYP/6-31G(d) level, namely, the activation free energy, ΔGact [ΔGact = G(TS) − G(R)], and reaction free energy, ΔGreac [ΔGreac = G(P) − G(R)] calculated at 298 K and 1 atm. In addition, the combined effect of the LA and α or β −OCH$_3$ substitution will be considered. In Table 5, ΔGact and ΔGreac for reactions 1−9 are collected.

As it was discussed previously, the Lewis acid, BH$_3$ or protonation (H$^+$), interacts with one of the lone pairs of O$_6$, forming a dative bond or an O−H bond, respectively.[32] Therefore, the effect of the Lewis acid can be viewed as a relative stabilization of the transition structure and the product with respect to the reactive. Therefore, both ΔGact and ΔGreac will be reduced to 32.60 and 13.55 kcal/mol in reaction 2 and 19.02 and −2.95 kcal/mol in reaction 3, respectively. The calculated ΔGact and ΔGreac for reaction 4 are 36.77 and 8.82 kcal/mol, respectively. This result is in agreement with both experimentally and computationally acknowledged conclusions[13] that the rate acceleration effect is due to α −OCH$_3$ substitution in the Nazarov cyclization. Interestingly, the ELF analysis predicts a stabilization of the transition structure and the product due to α −OCH$_3$ substitution, similar to the effect of the LA. Hence, both effects take place on different structures, and they can work in a cooperative way as it is observed from the calculations of ΔGact and ΔGreac for reactions 5, 26.80 and −2.68 kcal/mol, and 6, 11.15 and −26.26 kcal/mol, respectively.

Table 4. ELF Integrated Populations (in Electrons) for the Most Representative Basins of Reactive (R), Transition Structure (TS), and Product (P) for Reactions 1, 4, and 7

	R1	TS1	P1	R4	TS4	P4	R7	TS7	P7
V(C$_1$,C$_2$)	2.21	2.58	2.67	2.26	2.51	2.62	2.26	2.81	2.79
V(C$_2$,C$_3$)	1.63/1.78	2.64	2.12	1.77/1.87	2.72	2.17	1.76/1.84	2.51	2.18
V(C$_3$,C$_4$)			1.83			1.88			1.83
V(C$_3$)		0.37			0.24			0.59	
V(C$_4$)		0.36			0.5			0.45	
V(C$_4$,C$_5$)	1.63/1.78	2.65	2.12	1.68/1.78	2.66	2.04	1.79/1.67	2.55	2.12
V(C$_5$,C$_1$)	2.21	2.56	2.74	2.22	2.88	3.2	2.22	2.52	2.62
V(C$_1$,O$_6$)	2.35	2.15	2.05	2.34	2.14	1.95	2.25	2.14	2.07
V1,2(O$_6$)	2.62/2.62	2.75/2.75	2.82/2.82	2.61/2.65	2.79/2.7	2.99/2.79	2.7/2.64	2.8/2.75	2.85/2.77
V(C$_2$,O$_7$)				1.5	1.63	1.89			
V(C$_3$,O$_7$)							1.53	1.41	1.31
V(O$_7$,C)				1.41	1.42	1.49	1.38	1.34	1.32
V(O$_7$)				2.45/2.14	4.41	4.03	4.57	2.41/2.31	2.47/2.40

Table 5. Activation and Reaction Free Energies Calculated at 298 K and 1 atm (ΔGact and ΔGreac) Obtained at the B3LYP/6-31G(d) Calculation Level

reaction	R_1	R_2	LA	ΔGact	ΔGreac
1	−H	−H		42.83	27.64
2	−H	−H	BH_3	32.60	13.55
3	−H	−H	H^+	19.02	−2.95
4	$-OCH_3$	−H		36.77	8.82
5[a]	$-OCH_3$	−H	BH_3	26.80	−2.68
6	$-OCH_3$	−H	H^+	11.15	−26.26
7	−H	$-OCH_3$		43.41	38.11
8	−H	$-OCH_3$	BH_3	34.68	28.27
9	−H	$-OCH_3$	H^+	27.76	24.70

[a] Reaction 7 was calculated using the 6-31+G(d) basis set.

Experimental and theoretical calculations have shown the acceleration of the retro-Nazarov cyclization with electron-donor substituents in carbon β.[21] The B3LYP calculated ΔGact and ΔGreac of reaction 7 are 43.41 and 38.11 kcal/mol, respectively. The ELF analysis reveals that the electron-donating effect of β $-OCH_3$ substitution stabilizes the reactive and the TS (less) while the LA also stabilizes the TS and the product. Therefore, both effects are competitive on the reactive structure yielding smaller ΔGact but similar ΔGreac values for reactions 8, and 28.27 kcal/mol, and 9, 27.76 and 24.70 kcal/mol, respectively.

4. Conclusions

The forming/breaking bond processes and electronic rearrangements along the reaction path associated with the Nazarov cyclizations of penta-1,4-diene-3-one and derivatives have been studied in the framework provided by the topological analysis of the ELF together with CT. The presence of a Lewis acid (protonation $H^+$and BH_3) as well as an electron-donor substituent ($-OCH_3$) at α and β positions is taken into account using nine different reaction models. The main conclusions can be summarized as follows:

(i) The weights of the Lewis resonance structures have been calculated from ELF basin populations for penta-1,4-diene-3-one (R1) and its corresponding oxyallyl ring (P1).

(ii) The cyclization of R1 takes place following four different structural SSDs (I−IV) connected by three turning points (cusp1−fold1−cusp2). The first and most energetically demanding step for R1, reaction 1, corresponds to a polarization of the C−O bond, while the second step is associated with the electronic rearrangement among carbon−carbon bonds. The transition structure is located at the third SSD where the terminal carbon−carbon bond is not yet formed, and finally the ring closure process takes place.

(iii) The protonation of the ketone implies a modification of the ELF topology of the reactive (R3). Hence, the ELF topology of R3 corresponds to the second SSD of reaction 1, and the energetically expensive first SSD is avoided. The protonation of O_6 plays a decisive catalytic role, and it can be associated with the relative stabilization of the TS and product with respect to the reactive due to their larger zwitterionic character.

(iv) The analysis of ELF basin populations of reactives, transition structures, and products of reactions 1, 4, and 7 reveals the electron-donor capability of the $-OCH_3$ substituent at α and β positions, C_2 and C_3 carbon atoms, respectively. The basin corresponding to the lone pairs of O_7 can donate up to 0.58 e to the $V(C_{i=2,3}-O_7)$ bonding basin, depending on the electronic demands of the rearrangements taking place along the reaction path. The electron-donating effect goes in opposite directions for reactions 4 and 7.

(v) The variation of activation and reaction free energies observed for the combined effects of a Lewis acid (H^+, BH_3) and the α or β $-OCH_3$ substituents has been rationalized in terms of stabilization of the stationary points for reactions 1−9 due to the previously described electronic effects. The presence of Lewis acids and the presence of the α $-OCH_3$ substituent is cooperative, reducing greatly the activation free energy and yielding a clearly exergonic reaction. On the other hand, LA and β $-OCH_3$ act in a competitive way, decreasing the acceleration of the cyclization process.

Acknowledgment. This work was supported by the Ministerio de Ciencia y Tecnología (MCyT), DGICYT, BQU2003-04168-C03-03, and CTQ2006-15447-C02-01; Generalitat Valenciana, Projects GRUPOS03/176 and ACOMP06/122; and the Universitat Jaume I-Fundacio Bancaixa, Project P1.1B2004-20. V.P. thanks support by the Juan de la Cierva fellowship from the MCyT. The authors also are grateful to the Servei d'Informatica, Universitat Jaume I for a generous allotment of computer time. Dr. Luis Domingo is acknowledged for his comments on the manuscript.

Supporting Information Available: Optimized B3LYP/6-31G(d) or 6-31+G(d) for reaction 7; geometries, total energies (au), lowest frequency (cm^{-1}), zero-point energy correction, enthalpy, and free energy for the reactive, transition structure, product of reactions 1−9 are provided. This material is available free of charge via the Internet at http://acs.pubs.org.

References

(1) (a) Bader, R. F. W. *Acc. Chem. Res.* **1985**, *18*, 9−15. (b) Bader, R. F. W. *Atoms in Molecules. A Quantum Theory*; Claredon Press: Oxford U. K., 1990.

(2) Becke, A. D.; Edgecombe, K. E. *J. Chem. Phys.* **1990**, *92*, 5397−5403.

(3) Silvi, B.; Savin, A. *Nature* **1994**, *371*, 683−686.

(4) Shaik, S.; Danovich, D.; Silvi, B.; Lauvergnat, D. L.; Hiberty, P. C. *Chem.—Eur. J.* **2005**, *11*, 6358−6371.

(5) (a) Lepetit, C.; Silvi, B.; Chauvin, R. *J. Phys. Chem. A* **2003**, *107*, 464−473. (b) Santos, J. C.; Andres, J.; Aizman, A.; Fuentealba, P. *J. Chem. Theory Comput.* **2005**, *1*, 83−86. (c) Poater, J.; Duran, M.; Sola, M.; Silvi, B. *Chem. Rev.* **2005**, *105*, 3911−3947.

(6) Polo, V.; Andres, J.; Silvi, B. *J. Comput. Chem.* **2007**, *28*, 857−863.

(7) Krokidis, X.; Noury, S.; Silvi, B. *J. Phys. Chem. A* **1997**, *101*, 7277−7282.

(8) (a) Thom, R. *Structural Stability and Morphogenesis: An Outline of a General Theory of Models*; Benjamin: Reading, PA, 1975. (b) Poston, T.; Stewart, L. *Catastrophe Theory and its Applications*; Dover Publications, Inc.: Mineola, New York, 1996.

(9) Silvi, B. *J. Phys. Chem. A* **2003**, *107*, 3081−3085.

(10) (a) Berski, S.; Andres, J.; Silvi, B.; Domingo, L. R. *J. Phys. Chem. A* **2003**, *107*, 6014−6024. (b) Polo, V.; Andres, J.; Castillo, R.; Berski, S.; Silvi, B. *Chem.—Eur. J.* **2004**, *10*, 5165−5172. (c) Santos, J. C.; Andrés, J.; Aizman, A.; Fuentealba, P.; Polo, V. *J. Phys. Chem. A* **2005**, *16*, 3687−3693. (d) Santos, J. C.; Polo, V.; Andres, J. *Chem. Phys. Lett.* **2005**, *406*, 393−397. (e) Polo, V.; Andres, J. *J. Comput. Chem.* **2005**, *26*, 1427−1437. (f) Berski, S.; Andrés, J.; Silvi, B.; Domingo, L. R. *J. Phys. Chem. A* **2006**, *110*, 13939−13947.

(11) (a) Joubert, L.; Adamo, C. *J. Chem. Phys.* **2005**, *123*, 211103. (b) Joubert, L.; Pavone, M.; Barone, V.; Adamo, C. *J. Chem. Theory Comput.* **2006**, *2*, 1220−1227.

(12) (a) Marvell, E. N. *Thermal Electrocyclic Reactions*; Academic Press: New York, 1980; Vol. 43. (b) Ansari, F. L.; Qureshi, R.; Qureshi, M. L. *Electrocyclic Reactions*; Wiley: Weinheim, Germany, 1999. (c) Woodward, R. B.; Hoffmann, R. *The Conservation of Orbital Symmetry*; Verlag Chemie: Weinheim, Germany, 1970.

(13) Nazarov, I. N.; Zaretskaya, I. I. *Izv. Akad. Nauk. SSSR, Ser. Khim.* **1941**, 221−224.

(14) See the reviews: (a) Denmark, S. E. Nazarov and Related Cationic Cyclizations. In *Comprehensive Organic Synthesis*; Trost, B. M., Fleming, I., Paquette L. A., Eds.; Pergamon: Oxford, U. K., 1991; Vol. 5, pp 751−784. (b) Habermas, K. L.; Denmark, S. E.; Jones, T. K. The Nazarov Cyclization. In *Organic Reactions*; Paquette, L. A., Ed.; Wiley: New York, 1994; Vol. 45, pp 1−158.

(15) (a) Frontier, A. J.; Collison, C. *Tetrahedron* **2005**, *61*, 7577−7606. (b) Pellissier, H. *Tetrahedron* **2005**, *61*, 6479−6517.

(16) Liang, G. X.; Trauner, D. *J. Am. Chem. Soc.* **2004**, *126*, 9544−9545.

(17) (a) Wang, Y.; Arif, A. M.; West, F. G. *J. Am. Chem. Soc.* **1999**, *121*, 876−877. (b) Giese, S.; Kastrup, L.; Stiens, D.; West, F. G. *Angew. Chem., Int. Ed.* **2000**, *39*, 1970.

(18) (a) Smith, D. A.; Ulmer, C. W. *J. Org. Chem.* **1991**, *56*, 4444−4447. (b) Smith, D. A.; Ulmer, C. W. *Tetrahedron Lett.* **1991**, *32*, 725−728. (c) Smith, D. A.; Ulmer, C. W. *J. Org. Chem.* **1993**, *58*, 4118−4121. (d) Smith, D. A.; Ulmer, C. W. *J. Org. Chem.* **1997**, *62*, 5110−5115. (e) Faza, A. N.; Lopez, C. S.; Alvarez, R.; de Lera, I. R. *Chem.—Eur. J.* **2004**, *10*, 4324−4333. (f) Cavalli, A.; Masetti, M.; Recanatini, M.; Prandi, C.; Guarna, A.; Occhiato, E. G. *Chem.—Eur. J.* **2006**, *12*, 2836−2845.

(19) Even reagent-free Nazarov cyclizations have been proposed: Douelle, F.; Tal, L.; Greaney, M. F. *Chem. Commun.* **2005**, *5*, 660−662.

(20) (a) Denmark, S. E.; Habermas, K. L.; Hite, G. A. *Helv. Chim. Acta* **1988**, *71*, 168−194. (b) Tius, M. A. *Acc. Chem. Res.* **2003**, *36*, 284−290.

(21) (a) Harmata, M.; Lee, D. R. *J. Am. Chem. Soc.* **2002**, *124*, 14328−14329. (b) Harmata, M.; Schreiner, P. R.; Lee, D. R.; Kirchhoefer, P. L. *J. Am. Chem. Soc.* **2004**, *126*, 10954−10957.

(22) Frisch, M. J.; Trucks, G. W.; Schlegel, H. B.; Scuseria, G. E.; Robb, M. A.; Cheeseman, J. R.; Montgomery, J. A., Jr.; Vreven, T.; Kudin, K. N.; Burant, J. C.; Millam, J. M.; Iyengar, S. S.; Tomasi, J.; Barone, V.; Mennucci, B.; Cossi, M.; Scalmani, G.; Rega, N.; Petersson, G. A.; Nakatsuji, H.; Hada, M.; Ehara, M.; Toyota, K.; Fukuda, R.; Hasegawa, J.; Ishida, M.; Nakajima, T.; Honda, Y.; Kitao, O.; Nakai, H.; Klene, M.; Li, X.; Knox, J. E.; Hratchian, H. P.; Cross, J. B.; Bakken, V.; Adamo, C.; Jaramillo, J.; Gomperts, R.; Stratmann, R. E.; Yazyev, O.; Austin, A. J.; Cammi, R.; Pomelli, C.; Ochterski, J. W.; Ayala, P. Y.; Morokuma, K.; Voth, G. A.; Salvador, P.; Dannenberg, J. J.; Zakrzewski, V. G.; Dapprich, S.; Daniels, A. D.; Strain, M. C.; Farkas, O.; Malick, D. K.; Rabuck, A. D.; Raghavachari, K.; Foresman, J. B.; Ortiz, J. V.; Cui, Q.; Baboul, A. G.; Clifford, S.; Cioslowski, J.; Stefanov, B. B.; Liu, G.; Liashenko, A.; Piskorz, P.; Komaromi, I.; Martin, R. L.; Fox, D. J.; Keith, T.; Al-Laham, M. A.; Peng, C. Y.; Nanayakkara, A.; Challacombe, M.; Gill, P. M. W.; Johnson, B.; Chen, W.; Wong, M. W.; Gonzalez, C.; Pople, J. A. *Gaussian 03*, revision C.02; Gaussian, Inc.: Wallingford, CT, 2004.

(23) (a) Becke, A. D. *Phys. Rev. A: At., Mol., Opt. Phys.* **1988**, *38*, 3098−3100. (b) Becke, A. D. *J. Chem. Phys.* **1993**, *98*, 1372−1377. (c) Lee, C. T.; Yang, W. T.; Parr, R. G. *Phys. Rev. B: Condens. Matter Mater. Phys.* **1988**, *37*, 785−789.

(24) Hariharan, P. C.; Pople, J. A. *Theor. Chim. Acta* **1973**, *28*, 213−222.

(25) (a) Fukui, K. *J. Phys. Chem.* **1970**, *74*, 4161. (b) Fukui, K. *Acc. Chem. Res.* **1981**, *14*, 363−368.

(26) Gonzalez, C.; Schlegel, H. B. *J. Phys. Chem.* **1990**, *94*, 5523−5527.

(27) (a) Savin, A.; Becke, A. D.; Flad, J.; Nesper, R.; Preuss, H.; Vonschnering, H. G. *Angew. Chem., Int. Ed.* **1991**, *30*, 409−412. (b) Savin, A.; Jepsen, O.; Flad, J.; Andersen, O. K.; Preuss, H.; Vonschnering, H. G. *Angew. Chem., Int. Ed.* **1992**, *31*, 187−188. (c) Savin, A.; Nesper, R.; Wengert, S.; Fassler, T. F. *Angew. Chem., Int. Ed.* **1997**, *36*, 1809.

(28) Silvi, B. *J. Mol. Struct.* **2002**, *614*, 3−10.

(29) Noury, S.; Krokidis, X.; Fuster, F.; Silvi, B. *Comput. Chem.* **1999**, *23*, 597−604.

(30) Flükiger, P.; Lüthi, H. P.; Portmann, S.; Weber, J. *MOLEKEL 4.0*; J. Swiss Center for Scientific Computing: Manno, Switzerland, 2000.

(31) The same study along the IRC path was carried out for reaction 2 yielding an intermediate situation between 1 and 3; for the sake of clarity, the analysis of 2 is not discussed here.

(32) In the case of methoxy substitution at C_2, the BH_3 can interact with both oxygen atoms. The trans conformation with respect to the C_2 carbon atom has been chosen to analyze the Lewis acid effect on the keto group.

CT7000304